

Minimal and complete set of descriptors for IR-absorption spectra of liquid H₂-D₂ mixtures

Cite as: AIP Advances 10, 055108 (2020); <https://doi.org/10.1063/1.5111000>

Submitted: 28 May 2019 . Accepted: 15 April 2020 . Published Online: 05 May 2020

Robin Grössle , Beate Bornschein, Alexander Kraus, Sebastian Mirz, and Sebastian Wozniowski



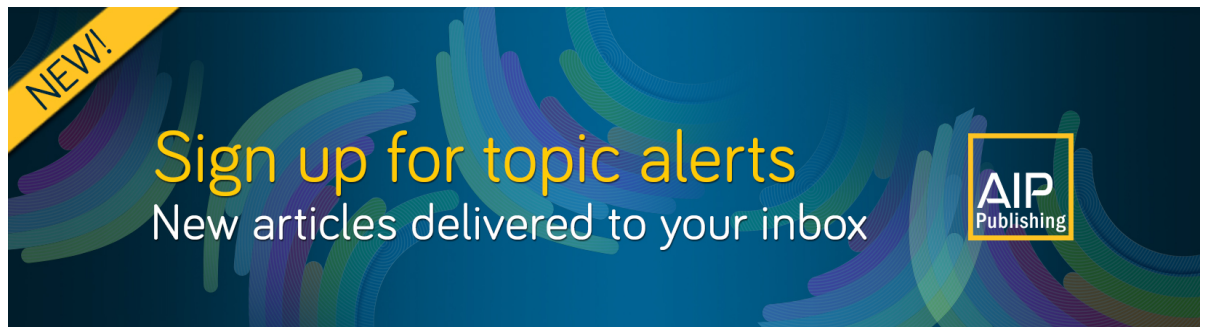
View Online



Export Citation



CrossMark



NEW!

Sign up for topic alerts
New articles delivered to your inbox

AIP
Publishing

Minimal and complete set of descriptors for IR-absorption spectra of liquid H₂-D₂ mixtures

Cite as: AIP Advances 10, 055108 (2020); doi: 10.1063/1.5111000

Submitted: 28 May 2019 • Accepted: 15 April 2020 •

Published Online: 5 May 2020



View Online



Export Citation



CrossMark

Robin Grössle,^{a)}  Beate Bornschein, Alexander Kraus, Sebastian Mirz, and Sebastian Wozniewski

AFFILIATIONS

Institute for Nuclear Physics, Tritium Laboratory Karlsruhe, Karlsruhe Institute of Technology, Hermann-von-Helmholtz-Platz 1, 76344 Eggenstein-Leopoldshafen, Germany

^{a)} Author to whom correspondence should be addressed: robin.groessle@kit.edu

ABSTRACT

The IR spectra of liquid hydrogen isotopologues ($Q_2 = \text{H}_2, \text{D}_2, \text{T}_2, \text{HD}, \text{HT}, \text{DT}$) are dominated by the interaction induced absorption. Therefore, the complexity tremendously increases with the number of different isotopologues in the sample. As we aim for a system independent calibration of IR absorption spectroscopy against all six isotopologues and three ortho-para ratios, we need a minimal and complete set of descriptors to predict the spectra and to decrease the needed calibration effort. For this, we grouped the absorption lines into three groups: absorption on monomers, phonons, and molecular dimers. In particular, molecular dimers contribute to the absolute number of absorption lines in the spectra of mixed isotopologues. To develop and test the set of descriptors, we make use of three spectra: a pure H₂ sample, a pure D₂ sample, and a mixed H₂-D₂ sample. We show a detailed analysis of these three spectra in the first and second vibrational branch in the range from 2000 cm⁻¹ to 9000 cm⁻¹. The set of descriptors found within this work can be used to identify and predict all lines in this range for liquid H₂-D₂ mixtures.

© 2020 Author(s). All article content, except where otherwise noted, is licensed under a Creative Commons Attribution (CC BY) license (<http://creativecommons.org/licenses/by/4.0/>). <https://doi.org/10.1063/1.5111000>

I. INTRODUCTION

The development of analytic systems and methods for tritium and other hydrogen isotopologues is a main research field at the Tritium Laboratory Karlsruhe (TLK). One of the methods under development is IR absorption spectroscopy for the concentration measurement of liquid hydrogen isotopologues at temperatures between 15 K and 25 K.²⁻⁴ This method can be used for in-line and real-time process monitoring of cryogenic distillation columns or the measurement of the ortho/para ratio of the homonuclear hydrogen isotopologues (H₂, D₂, and T₂).

We are aiming for a full calibration of the IR absorption spectra of liquid hydrogen isotopologue mixtures against all six concentrations ($Q_2 = \text{H}_2, \text{D}_2, \text{T}_2, \text{HD}, \text{HT}, \text{DT}$) and the three ortho/para ratios. The first calibration for H₂, D₂, and HD mixtures with fixed ortho/para ratios leads to a total accuracy of better than 5%.²³

Previous studies of absorption spectra of liquid H₂ and D₂ for different ortho/para ratios and temperatures show a strong influence of these parameters on the first vibrational branch.^{5,6} This limits

the trueness of our calibration. Additionally, for isotopologue mixtures, molecular dimers do complicate the IR absorption spectra tremendously.¹ For the interpretation of the experimental data, we aim for a minimal and complete set of descriptors for the IR spectra of liquid hydrogen isotopologue mixtures. This will be crucial for the upcoming measurement campaigns with the tritium compatible setup that is under construction at the TLK,⁴ where we plan to extend this calibration to all six hydrogen isotopologues and variable ortho/para ratios. To extract the minimal and complete set of descriptors, we studied the IR absorption spectra of pure H₂ and D₂ liquid samples, and a H₂-D₂ mixture.

II. THEORETICAL OVERVIEW

As diatomic molecules, the hydrogen isotopologues undergo rotational and vibrational excitations by the absorption of an infrared photon.

The hydrogen isotopologues follow the vibrational selection rule of $\Delta v \geq 0$. $\Delta v = 0$ transitions create the pure rotational transition

spectrum; $\Delta\nu = 1$ constitutes the common ro-vibrational “fundamental absorption” spectrum; higher vibrational excitation $\Delta\nu \geq 2$ represent the “overtone bands” with transition probabilities at least one to two orders of magnitude lower than that for $\Delta\nu = 1$. Only the (small) anharmonicity in the molecular potential makes these transition probabilities non-vanishing.⁷

The rotational selection rules of the hydrogen isotopologues for IR absorption differ from the general selection rules for diatomic molecules due to the ortho/para modifications of the homonuclear hydrogen molecules. Infrared absorption follows the rotational selection rule of $\Delta J = 0, \pm 1$ for diatomic molecules. For homonuclear hydrogen isotopologues (H_2 , D_2 , T_2), the $\Delta J = \pm 1$ transition is forbidden due to the forbidden ortho \leftrightarrow para transition. For the heteromolecular hydrogen isotopologues (HD, HT, and DT), these transitions are suppressed by the vanishing inertia tensor along the main axis θ_z .^{8,9}

This implies that only “pure vibrational” transitions ($\Delta\nu \geq 1$; $\Delta J = 0$) could be observed, without rotational companion lines with $\Delta J \neq 0$. However, experimental observations contradict this by exhibiting clear rotational S-branch lines;^{10–18} for an explanation of the related selection rule $\Delta J = +2$, see further below.

Theory discusses different mechanisms to solve this contradiction; van Kranendonk gave the first overview on this in 1957, which was followed by Ref. 8, 19, and 20. These mechanisms are mainly based on the van der Waals interactions between hydrogen molecules and enable the formation of oligomers. Parameters of these bonds, such as binding potentials, are investigated to the present day.^{9,12,21–24} Already the simplest oligomer, the dimer, offers an additional rotational and vibrational quantum number^{21,23} to explain the rotational splitting in the IR absorption spectra and the observed selection rules of $\Delta\nu \geq 0$ and $\Delta J = 0, \pm 2$.

III. EXPERIMENTAL STRATEGY

For the present work, we studied three different samples in the liquid phase: pure H_2 , pure D_2 , and a mixture of both (see Table I).

At low temperatures of about 20 K, almost only the ground state of the molecules is expected to be occupied. Due to the forbidden ortho \leftrightarrow para transition of the homonuclear isotopologues, the sum of the odd J states and the sum of even J states are almost constant in time. Therefore, the first excited rotational state $J = 1$ is occupied in the case of a sufficiently fast cool down. The J_1 to J_0

TABLE I. Compositions of the investigated hydrogen samples. Samples a and b are pure samples; the indicated concentrations are the manufacturer’s data. The D_2 calibration gas has an atomic purity of 99.7%, which corresponds to a fraction of 0.6% HD. Sample c has been mixed within the experimental setup. Since the ideal gas law has been used and the liquefaction process influences the composition, it is difficult to deduce accurate values; the actual composition has been measured by Raman spectroscopy.

Sample	c_{H_2}	c_{HD}	c_{D_2}	
A	D_2	0	0.006	0.994
B	H_2	1	0	0
C	$H_2 + D_2$	0.429	0.003	0.568

ratio is 3:1 for H_2 (6:3 for D_2) directly after the liquefaction.²⁵ This ratio changes by natural equilibration, which can be neglected due to its long conversion times (>days^{26,27}). For this work, the precise ortho/para ratio is not needed for the discussion. However, it is a major systematic uncertainty for the calibration of an IR absorption based concentration-measurement and requires a separate treatment.^{3,4} Higher energetic J states ($J > 1$) are negligibly occupied at the low temperatures of the liquid phase, therefore no $\Delta J = -2, \dots$ transitions are expected for both homonuclear and heteronuclear hydrogen isotopologues.

The present study does not use the common method of comparison for calculation with the measured line position, which is limited to the broad lines in the liquid phase (see Sec. V A). Instead, we use a twofold approach. First, we check for missing lines predicted by the current set of descriptors to verify or falsify these. Second, we investigate lines in a H_2 – D_2 mixture that are not present in pure H_2 or pure D_2 spectra (see Table I for the composition of all investigated samples). HD as the origin of these additional lines is ruled out by a reference measurement by Raman spectroscopy in the gas phase before the liquefaction and after the re-vaporization of the liquid sample having completed the IR-measurements. Therefore, these additional lines must be associated with heteromolecular hydrogen dimers. A rough analysis of the line positions of these lines also makes it possible to verify or reject specific selection rules.

IV. EXPERIMENTAL DETAILS

As described by Größle *et al.*,² the hydrogen isotopologues are liquefied in an infrared sample cell with a volume of 100 ml and an absorption length of 4.5 cm. The sample cell operates at a pressure up to 3.5 bars and is equipped with sapphire view-ports (diameter 3.2 cm). The sample cell is cooled by gaseous helium provided by a helium refrigeration system with a cooling power of 250 W at 16 K helium temperature. It is surrounded by an insulation vacuum container with a pressure $<10^{-4}$ mbar, which is also equipped with sapphire view-ports.

The sample temperatures are between 19 K and 21 K. Infrared absorption spectra are obtained with a Bruker Tensor 27 FT-IR spectrometer with a resolution of 0.9 cm^{-1} combined with an external liquid nitrogen cooled HgCdTe detector.

A. Measurement description

The typical measurement consists of several steps. First, a pure H_2 , D_2 , or a mixed H_2 – D_2 gas sample is prepared. In the case of a mixed sample, its composition is measured by Raman spectroscopy as described in Refs. 28 and 29. The isotopologue concentrations of the samples of the present analysis are listed in Table I. Second, the sample cell is cooled below the boiling point of the gas mixture and the condensation process starts. Third, the sample cell is constantly cooled and filled with liquid by condensation, which takes about 8 h. Fourth, IR absorption spectra are taken for up to 30 min. Fifth, the liquid is evaporated and the sample cell is evacuated to take IR reference spectra with the empty sample cell.

For the mixed H_2 – D_2 sample, another Raman measurement is taken in the gas phase. By this, the formation of HD during the measurement process can be monitored and in this case excluded.

B. Data analysis

The recorded infrared absorption spectra are evaluated in four steps, as described by Größle *et al.*² The first step is a Fourier transformation and corrections to the 15–25 recorded sample and reference interferograms applied by the OPUS software from Bruker. Second, the recorded transmittance spectra are normalized to their intensity at 2500 cm^{-1} and treated with an elliptical rolling circle filter as described by Mikhailyuk and Razzhivin.³⁰ We adapted this filter procedure by taking values for independent filter radii for the wavenumber $\tilde{\nu}$ and intensity I as $r_{\tilde{\nu}} = 2500\text{ cm}^{-1}$ and $r_I = 2.5$, respectively. This filter step removes the influence from background effects, such as the varying detector sensitivity, source fluctuations, and the influence of the surface reflection between the sample and the sapphire window. Third, each of the sample spectra is divided by the associated reference spectra, the resulting transmittance spectra are averaged, and the 68.2th percentile is calculated as an estimation for the square root of the variance. Fourth, the decadic absorbance $A = -\log_{10}(T)$ is calculated from the transmittance T and spectral lines are integrated over the intervals listed in Table III.

C. Calculation of line positions and occupational numbers

For the interpretation of the recorded spectra, the molecular energy levels are calculated based on molecular constants for the gas phase published by Huber and Herzberg and the calculation given in their publication.³¹ The transitions are then derived as the energy difference between the initial and the final states, where the initial state is always in the vibrational ground state ($v = 0$) and in the rotational ground state ($J = 0$) or the first excited state ($J = 1$). The final state is then selected based on the initial state by the selection rules $\Delta v \geq 0$ and $\Delta J = 0, 2$. This approximation is valid under the assumption that the energy levels and, therefore, the rotational and vibrational quantum numbers of hydrogen molecules of the gaseous phase are still valid in the liquid phase and the corrections are small compared to the expected line width.³² The energies of dimer transitions are calculated as the combination of the two monomer transitions.¹² Additional excitation energies of a possible dimer rotation are neglected.

Transitions are shortly denoted as $\Delta J_{\Delta v}(J'')$, where ΔJ is the rotational excitation expressed by letters Q, R, and S (Q corresponds to $\Delta J = 0$, R to $\Delta J = 1$, and S to $\Delta J = 2$) and J'' is the initial rotational state. Δv represents the vibrational excitation, where the initial vibrational state is $v = 0$.

At the cryogenic temperatures encountered here, no measurable population is found in any higher vibrational state. The occupational numbers can be calculated by the energy level of the initial states and the Boltzmann distribution, where one has to take into account the spin degeneracy of the nuclei. This is 3:1 (odd J'' , even J'') for H_2 and 6:9 for D_2 . In addition, the slow conversion between ortho and para has to be considered.³³ This is done by executing the Boltzmann distribution in two iterations. First, with a sample temperature that corresponds to the ortho–para equilibrium. We used 300 K. From this first iteration one will get the ortho–para ratio (sum of the odd or even states), here, almost the nuclear spin degeneracy for the corresponding isotopologue. This

ratio is then maintained, and the Boltzmann distribution is executed a second time. This time separately for the odd states and then for the even states, where the normalization factor for the odd and the even states is used from the first iteration. From this, one simulates that the transitions only occur within the even or within the odd states during the cool down from room temperature to around 20 K.

From this, significant population is only found for the rotational levels $J'' = 0$ and $J'' = 1$. In addition, the transition lines are indexed (as superscript) with the associated isotopologue, equally for monomers and dimers. For example, $S_0^{H_2}(1)Q_1^{D_2}(0)$ indicates a mixed isotopologue dimer exhibiting an ortho-S-transition (on H_2) and an ortho-Q-transition (on D_2).³⁴ Selected strong transitions are summarized in Tables II and III, with a full list of all calculated transitions provided in the supplementary material.

TABLE II. Overview of the dominant transitions in the fundamental vibrational band of liquid D_2 (sample a), H_2 (sample b), and mixtures (sample c). The dominant transitions are given with their calculated position ν_0 and calculated occupational number N . In the first vibrational branch, the transitions cannot be spectrally separated, so calculating the intensities and the center of gravity is strongly dependent on the selection of integration ranges.

Transition	Calculation	
	$\nu_0(\text{cm}^{-1})$	$N(I)$
	Sample (a)	
$Q_1^{D_2}(1)$	2989.7	0.33
$Q_1^{D_2}(0)$	2991.9	0.67
$S_0^{D_2}(0)Q_1^{D_2}(1)$	3168.7	0.44
$S_0^{D_2}(0)Q_1^{D_2}(0)$	3170.9	0.89
$S_0^{D_2}(1)Q_1^{D_2}(1)$	3287.1	0.22
$S_0^{D_2}(1)Q_1^{D_2}(0)$	3289.3	0.44
	Sample (b)	
$Q_1^{H_2}(1)$	4152.4	0.75
$Q_1^{H_2}(0)$	4158.6	0.25
$S_0^{H_2}(0)Q_1^{H_2}(1)$	4506.7	0.38
$S_0^{H_2}(0)Q_1^{H_2}(0)$	4512.8	0.13
$S_0^{H_2}(1)Q_1^{H_2}(1)$	4739.1	1.12
$S_0^{H_2}(1)Q_1^{H_2}(0)$	4745.2	0.38
	Sample (c)	
$S_0^{H_2}(0)Q_1^{D_2}(1)$	3343.9	0.04
$S_0^{H_2}(0)Q_1^{D_2}(0)$	3346.1	0.08
$S_0^{H_2}(1)Q_1^{D_2}(1)$	3576.3	0.12
$S_0^{H_2}(1)Q_1^{D_2}(0)$	3578.5	0.25
$S_0^{D_2}(0)Q_1^{H_2}(1)$	4331.4	0.25
$S_0^{D_2}(0)Q_1^{H_2}(0)$	4337.6	0.08
$S_0^{D_2}(1)Q_1^{H_2}(1)$	4449.9	0.12
$S_0^{D_2}(1)Q_1^{H_2}(0)$	4456.0	0.04

TABLE III. Overview of the dominant transitions in the first overtone band of liquid D₂ (sample a), H₂ (sample b), and mixtures (sample c). Besides, the line denomination and the calculated position ν_0 and calculated occupational number N , the integration range, the measured line centroid ν_0 , absorbance A , and the 1σ (68.2%) confidence level are given.

Calculation			Measurement			
Transition	ν_0 (cm ⁻¹)	N	Int. range (cm ⁻¹)	ν_0 (cm ⁻¹)	A (cm ⁻¹)	$Q_{0.682}$ (%)
Q ₂ ^{D2} (1)	5855.8	0.33	5825–5943	5865.0	0.43	2.5
Q ₂ ^{D2} (0)	5860.1	0.67				
Q ₁ ^{D2} (1)Q ₁ ^{D2} (1)	5979.4	0.11	5943–6001	5976.7	1.47	0.4
Q ₁ ^{D2} (1)Q ₁ ^{D2} (0)	5981.6	0.44				
Q ₁ ^{D2} (0)Q ₁ ^{D2} (0)	5983.7	0.44				
S ₀ ^{D2} (0)Q ₂ ^{D2} (1)	6034.8	0.44	6001–6102	6039.7	2.87	0.5
S ₀ ^{D2} (0)Q ₂ ^{D2} (0)	6039.1	0.89				
S ₀ ^{D2} (1)Q ₂ ^{D2} (1)	6153.2	0.22	6102–6236	6156.9	9.79	0.3
Q ₁ ^{D2} (1)S ₁ ^{D2} (0)	6154.1	0.44				
Q ₁ ^{D2} (0)S ₁ ^{D2} (0)	6156.3	0.89				
S ₀ ^{D2} (1)Q ₂ ^{D2} (0)	6157.5	0.44				
Q ₁ ^{D2} (1)S ₁ ^{D2} (1)	6266.1	0.22	6236–6300	6263.4	1.86	0.6
Q ₁ ^{D2} (0)S ₁ ^{D2} (1)	6268.2	0.44				
Sample (b)						
Q ₂ ^{H2} (1)	8062.2	0.75	8048–8106	8070.7	0.82	12.6
Q ₂ ^{H2} (0)	8074.4	0.25				
Q ₁ ^{H2} (1)Q ₁ ^{H2} (1)	8304.9	0.56	8268–8317	8300.6	3.00	16.2
Q ₁ ^{H2} (1)Q ₁ ^{H2} (0)	8311.0	0.38				
Q ₁ ^{H2} (0)Q ₁ ^{H2} (0)	8317.1	0.06				
S ₀ ^{H2} (0)Q ₂ ^{H2} (1)	8416.4	0.38	8400–8450	8420.3	0.40	0.0
S ₀ ^{H2} (0)Q ₂ ^{H2} (0)	8428.7	0.13				
Q ₁ ^{H2} (1)S ₁ ^{H2} (0)	8646.8	0.38	8615–8690	8644.9	1.37	31.8
S ₀ ^{H2} (1)Q ₂ ^{H2} (1)	8648.8	1.12				
Q ₁ ^{H2} (0)S ₁ ^{H2} (0)	8653.0	0.13				
S ₀ ^{H2} (1)Q ₂ ^{H2} (0)	8661.1	0.38				
Q ₁ ^{H2} (1)S ₁ ^{H2} (1)	8860.9	1.12	8830–8890	8857.2	1.95	23.4
Q ₁ ^{H2} (0)S ₁ ^{H2} (1)	8867.0	0.38				
Sample (c)						
S ₀ ^{H2} (0)Q ₂ ^{D2} (1)	6210.0	0.04	6102–6236	6157.9	2.90	1.2
S ₀ ^{H2} (0)Q ₂ ^{D2} (0)	6214.3	0.08				
S ₀ ^{H2} (1)Q ₂ ^{D2} (1)	6442.4	0.12	6412–6473	6444.4	0.16	5.3
S ₀ ^{H2} (1)Q ₂ ^{D2} (0)	6446.7	0.25				
Q ₁ ^{D2} (1)Q ₁ ^{H2} (1)	7142.1	0.12	7105–7200	7139.8	1.35	0.6
Q ₁ ^{D2} (0)Q ₁ ^{H2} (1)	7144.3	0.25				
Q ₁ ^{D2} (1)Q ₁ ^{H2} (0)	7148.3	0.04				
Q ₁ ^{D2} (0)Q ₁ ^{H2} (0)	7150.4	0.08				
S ₁ ^{D2} (0)Q ₁ ^{H2} (1)	7316.8	0.25	7275–7328	7311.3	1.74	1.1
S ₁ ^{D2} (0)Q ₁ ^{H2} (0)	7322.9	0.08				
S ₁ ^{D2} (1)Q ₁ ^{H2} (1)	7428.8	0.12	7395–7450	7424.9	0.35	4.8

TABLE III. (Continued.)

Calculation			Measurement			
Transition	ν_0 (cm ⁻¹)	N	Int. range (cm ⁻¹)	ν_0 (cm ⁻¹)	A (cm ⁻¹)	$Q_{0.682}$ (%)
S ₁ ^{D2} (1)Q ₁ ^{H2} (0)	7434.9	0.04				
Q ₁ ^{D2} (1)S ₁ ^{H2} (0)	7484.1	0.04	7450–7493	7478.7	0.50	2.8
Q ₁ ^{D2} (0)S ₁ ^{H2} (0)	7486.3	0.08				
Q ₁ ^{D2} (1)S ₁ ^{H2} (1)	7698.1	0.12	7673–7725	7695.5	0.73	3.3
Q ₁ ^{D2} (0)S ₁ ^{H2} (1)	7700.3	0.25				
S ₀ ^{D2} (0)Q ₂ ^{H2} (1)	8241.2	0.25	8220–8268	8245.1	0.45	9.9
S ₀ ^{D2} (0)Q ₂ ^{H2} (0)	8253.5	0.08				
S ₀ ^{D2} (1)Q ₂ ^{H2} (1)	8359.6	0.12	n.o.			
S ₀ ^{D2} (1)Q ₂ ^{H2} (0)	8371.9	0.04	n.o.			

V. EXPERIMENTAL RESULTS

As a primary result, the analysis procedure delivers three sets of spectra one for each of the pure H₂, D₂, and the mixed H₂–D₂ samples (see Figs. 1 and 2).

A. Spectral resolution and line broadening

The spectral resolution of our setup is 0.9 cm⁻¹ according to the manufacturer. In the gas phase,³⁵ this is enough to resolve almost all ro-vibrational spectral features for H₂, D₂, and mixtures. In the liquid phase, there is a severe line broadening due to which many spectral features cannot be resolved. A comparison of water vapor absorption lines and those of liquid H₂ can be found in the [supplementary material](#). This demonstrates that the resolution of our setup is not the limiting factor to resolve all the spectral features, but it is limited due to the line-broadening in the liquid phase.

In the end, our analysis shows that it is not possible to separately analyze $Q_{\Delta\nu}(0)$ and $Q_{\Delta\nu}(1)$ since the difference between these lines is equal to or much smaller than the typical linewidth. For D₂, Q₁(1) and Q₁(0) are separated by 2.2 cm⁻¹, and at $\Delta\nu = 2$, they are separated by 4.3 cm⁻¹. For H₂, the line-spacing is 6.2 cm⁻¹ in the first vibrational branch and 12.2 cm⁻¹ in the second. This is due to the low rotational anharmonicity contribution and could be resolved in the gas phase. For the liquid phase, these branches cannot be separated easily. However, the separation for H₂ is big enough to deconvolute the two contributions, especially when investigating varying ortho–para ratios, which is beyond the scope of this paper. Therefore, we indicate these lines by denoting Q₁(1) and Q₁(0) as Q₁(0, 1). At the same time, S _{$\Delta\nu$} (0) and S _{$\Delta\nu$} (1) are well-separated due to the rotational energy being proportional to $J(J + 1)$ in the first order.

B. First vibrational branch

1. First vibrational branch of H₂ and D₂

The first vibrational branch of D₂ (2900–4000 cm⁻¹), shown in Fig. 1, can be sufficiently described by a combination of monomer,

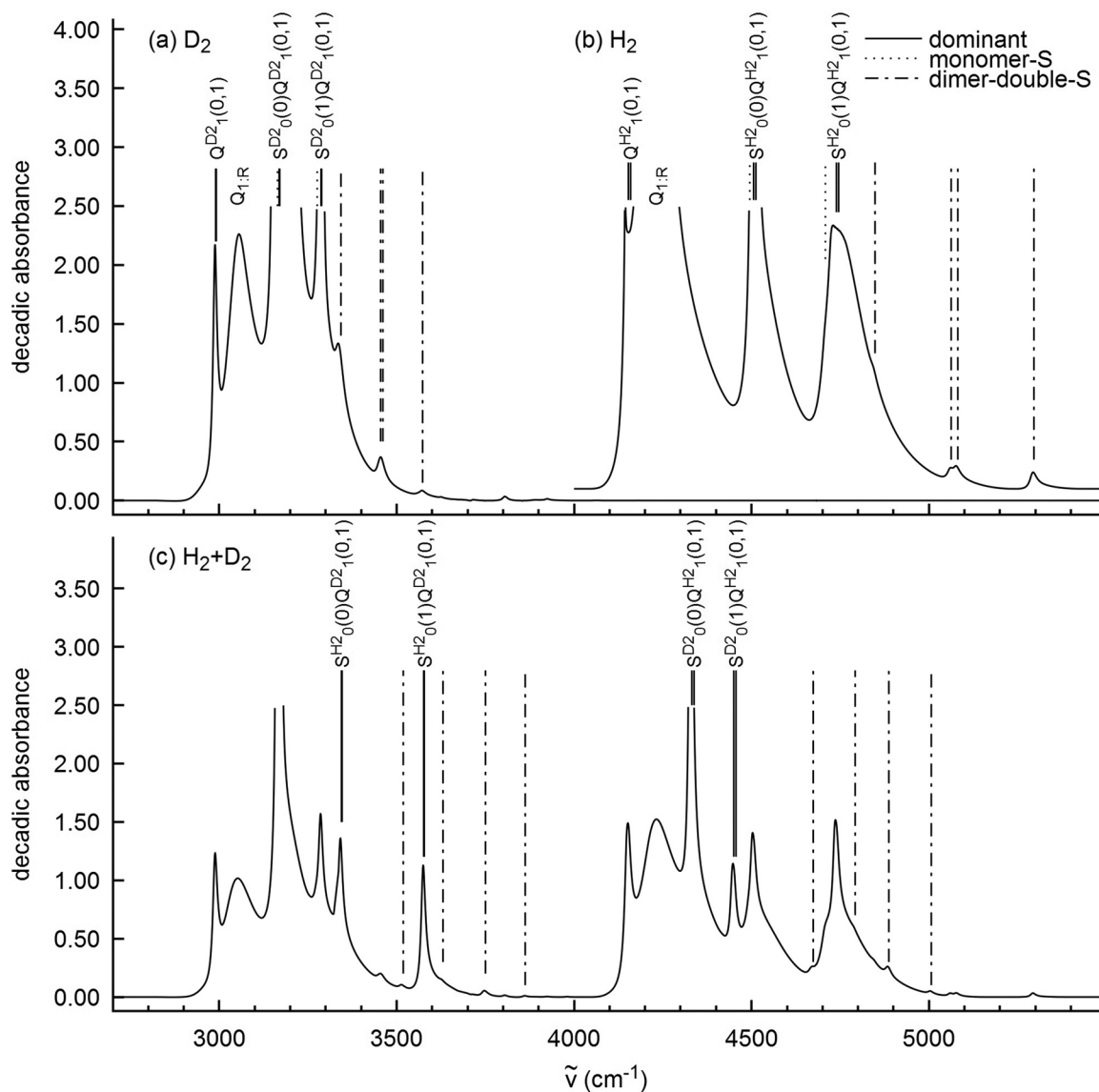


FIG. 1. IR absorption spectra of liquid hydrogen isotopologues (first vibrational branch). (a) D_2 , (b) H_2 (with an offset of 0.05), and (c) $H_2 + D_2$ mixture (see Table I). Calculated line positions are indicated: solid lines represent dominant transitions, dotted lines represent suppressed quadrupole monomer S transitions, and dashed-dotted lines represent suppressed dimer double-S transitions.

dimer, and phonon transitions. For the absorbance spectra, see Fig. 1 and Table II for a list of calculated dominant transitions.

The pure vibrational monomer transitions $Q_1(0, 1)$ give the lowest energetic lines close to 3000 cm^{-1} . A $50\text{--}100\text{ cm}^{-1}$ higher wavenumber exhibits the phonon transition [labeled $Q_{1,R}(0, 1)$]. This broad line is followed by the combined rotational and vibrational transitions labeled as $S_0(0)Q_1(0, 1)$ (at 3200 cm^{-1}) and $S_0(1)Q_1(0, 1)$ (at 3300 cm^{-1}). These absorption lines demonstrate again that the ortho ($J = 0$) and para ($J = 1$) transitions split into well-separated lines only if a rotation is located on the particular

molecule. In a pure vibrational excitation, these lines are not separately visible. In addition, the monomer $S_1(0)$ and the corresponding dimer transition $S_0(0)Q_1(0, 1)$ [and as well for $S_1(1)$] are not separately visible in the first vibrational branch. This is caused by the high decadic absorbance of more than 2.5, which exceeds the dynamic range of our setup and the liquid phase that broadens the lines (see also Sec. V A).

In addition, the spectrum shows four dimer double-S transitions whose integral absorbance is one to two orders of magnitude smaller than for the aforementioned transitions. First, the line at

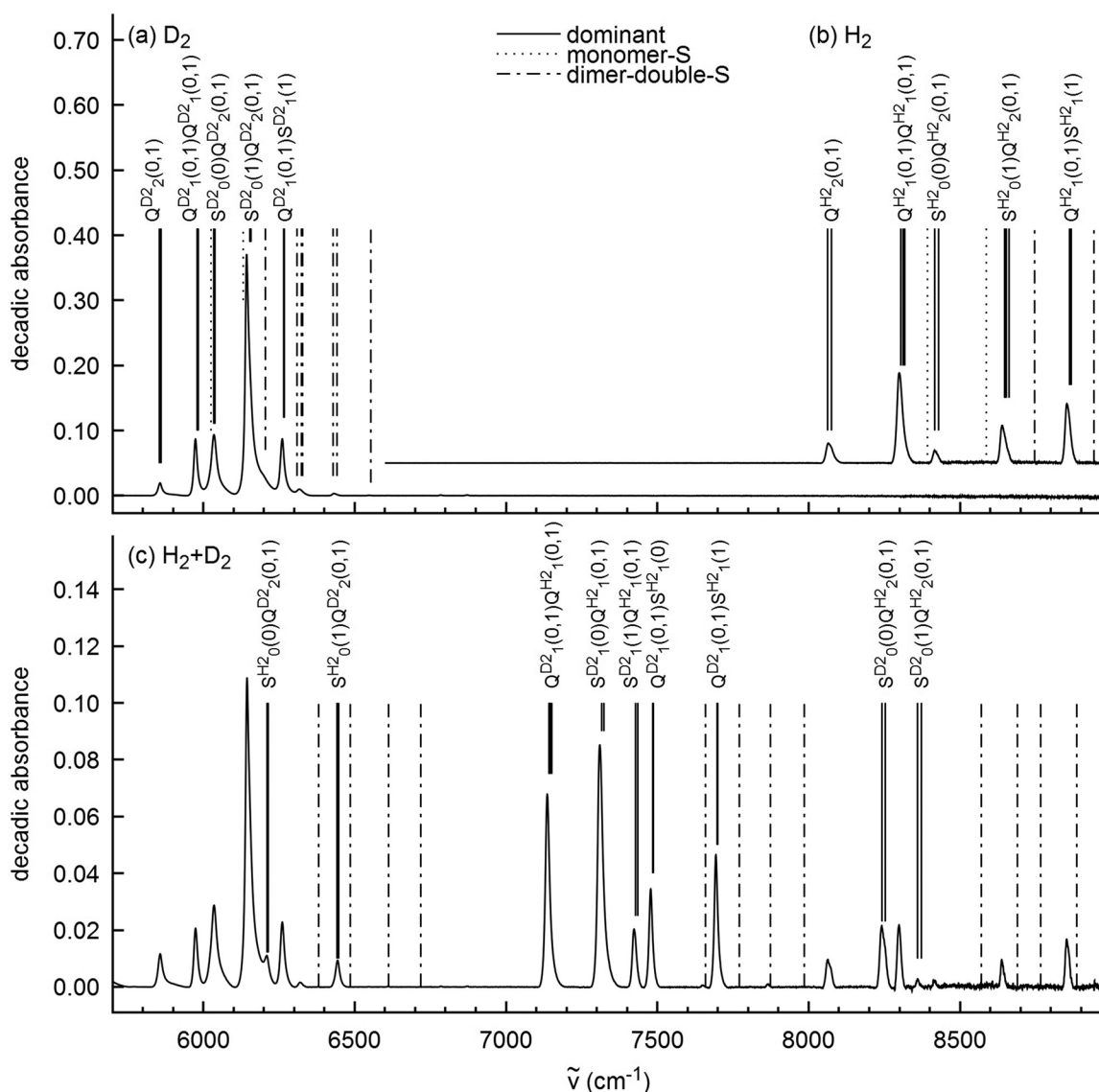


FIG. 2. IR absorption spectra of liquid hydrogen isotopologues (second vibrational branch). (a) D_2 , (b) H_2 (with an offset of 0.05), and (c) $H_2 + D_2$ mixture. Annotations as in Fig. 1.

about 3350 cm^{-1} is a double-S excitation of a D_2 ortho ($J = 0$) dimer $S_1(0)S_0(0)$. Second and third, at approximately 3450 cm^{-1} , there are the two excitations of an ortho/para dimer [$S_1(1)S_0(0)$] and [$S_1(0)S_0(1)$]. The splitting of these lines is caused by the location of the vibrational excitation on either the ortho or on the para molecule. Fourth, the transition at $\sim 3550\text{ cm}^{-1}$ corresponds to the para-para dimer $S_1(1)S_0(1)$. The integral absorbance of these four double-S transitions is much lower than that of the single-S-transitions. However, giving precise values is difficult since they are located on the high energy flank of the $S_0(1)Q_1(0, 1)$ line, which leads to a strong curvature of the background for the double-S transitions. However, when aiming for an ortho-para calibration, one should

look deeper into these four transitions since here the transitions corresponding to para-para, ortho-para, and ortho-ortho dimers are well-separated from each other.

The structure of the H_2 spectrum is very similar. However, the double S transition on the ortho/para dimer shows a better separation due to the lower rotational moment of inertia compared to the D_2 spectrum. Therefore, they should be even more useful for ortho-para studies.

2. First vibrational branch of the H_2 - D_2 mixture

Figure 1(c) shows the spectrum of the mixed sample. All lines of the pure H_2 - D_2 spectra are also visible, so only the additional lines

that are predicted by the selection for heteromolecular dimers are indicated in the spectrum.

In the D_2 branch, two relatively strong new lines, indicated by solid lines, are visible. These $S_0^{H_2}(0)Q_1^{D_2}(0,1)$ and $S_0^{H_2}(1)Q_1^{D_2}(0,1)$ lines can be associated with a rotational excitation on the para or the ortho H_2 molecule and a vibrational excitation on the D_2 molecule. These lines are shifted to higher wavenumbers compared to the corresponding pure D_2 dimer transitions caused by the lower rotational moment of inertia of the H_2 molecule.

In the H_2 branch, similar lines can be observed, which originate from the same mechanism. However, in this branch, they are shifted to lower wavenumbers with respect to the pure H_2 dimers. In addition, for this mixed sample, four additional lines are visible in each branch. Similar to the pure spectra, these lines are caused by double-S transitions of heteromolecular dimers.

C. Second vibrational branch

The overall structure of the second vibrational branch (Fig. 2) is quite similar to the first vibrational branch. Each branch of the pure samples begins with the pure vibrational monomer excitation $Q_2(0,1)$, followed by combined ro-vibrational transitions (see Table III).

The phonon excitations are hardly visible, which is a consequence of our background reduction. In the case of the D_2 branch, the residue of the phonon excitation can be seen on the high energy flank of the pure vibrational excitation at $\sim 5900\text{ cm}^{-1}$. However, there are two main differences to the first vibrational branch. First, the lines are better separated than in the first vibrational branch. Second, the vibrational excitation of $\Delta\nu = +2$ can be split to two molecules in a dimer. This directly leads to a pure vibrational dimer line Q_1Q_1 . For the homomolecular dimer, this line is the combination of the three excitations $Q_1(0)Q_1(0)$, $Q_1(0)Q_1(1)$, and $Q_1(1)Q_1(1)$. However, the splitting of the $Q_2(0,1)$ and $Q_1(0,1)$ $Q_1(0,1)$ lines directly reveals the an-harmonic vibrational potential. For the heteromolecular dimer, it is a combination of four excitations since $Q_1^{D_2}(0)Q_1^{H_2}(1)$ and $Q_1^{D_2}(1)Q_1^{H_2}(0)$ are distinguishable.

The dimer single S-transitions are split into four groups. Two with the rotational excitation on one molecule and the vibration on the other $S_0(0)Q_2(0,1)$ and $S_0(1)Q_2(0,1)$, and two where the vibrational excitation is split to both molecules $S_1(0)Q_1(0,1)$ and $S_1(1)Q_1(0,1)$. Similar to the pure vibrational excitations, the an-harmonic vibrational potential shifts the position of the S_1Q_1 lines to higher wavenumbers compared to those of S_0Q_2 . By this, the homomolecular $S_0(1)Q_2(0,1)$ and $S_1(0)Q_1(0,1)$ transitions overlap and cannot be separated. Therefore, only three lines are observed for these four groups.

1. Dimer double S transitions in the second vibrational branch

Double-S transitions are also suppressed in the second vibrational branch. In the region between 6400 cm^{-1} and 6600 cm^{-1} of the D_2 sample (see Fig. 3), double-S transitions are predicted and can be identified in the spectrum around 6550 cm^{-1} . They occur with a maximum peak height of 0.5×10^{-5} to 3.0×10^{-5} and an integral absorbance of 0.05 cm^{-1} . This corresponds to suppression by one

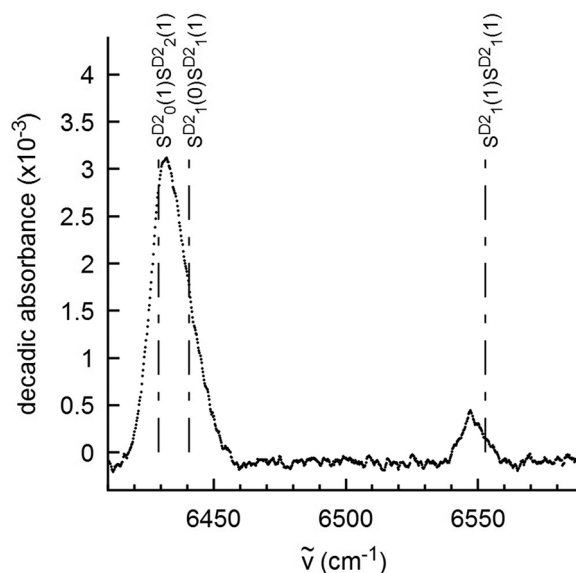


FIG. 3. IR spectrum of liquid D_2 of double S-transitions in the second vibrational branch. Calculated line positions are indicated by the annotated dashed-dotted lines, for details see text.

order of magnitude compared to the Q_2 monomer transition (integral absorbance of 0.43 cm^{-1} see Table III) and by a factor of 200 compared to dimer transitions. A precise quantification of this suppression is again difficult due to the overlapping lines. The same is true for heteromolecular dimers like in Fig. 4.

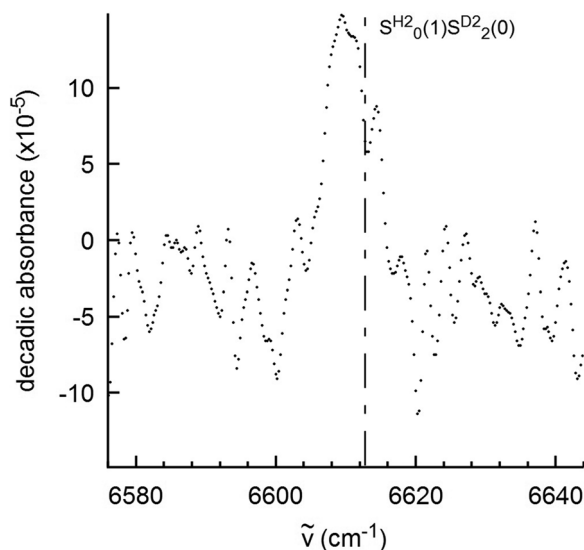


FIG. 4. IR spectrum of the heteromolecular dimer double-S-transition in the second vibrational branch. The calculated line position is indicated by the annotated dashed-dotted line; for further details, see text.

2. Monomer S-transitions

According to the fundamental selection rules of $\Delta J = 0, +1$, monomer S-transitions should be forbidden for dipole transitions, but not for quadrupole transitions. In the first vibrational branch, it is impossible to resolve the S_1 monomer and the S_0Q_1 dimer transitions due to the spectral broadening in the liquid phase. Just to remind, in the gas phase this can be resolved like shown by McKellar *et al.*^{12,35,36} For the second vibrational branch, the observed broadening is significantly smaller, and, therefore, it is possible to separate S_2 and S_0Q_2 transitions.

The $S_2(1)$ transition is expected between 8580 cm^{-1} and 8600 cm^{-1} (see Fig. 5). Our recorded spectrum shows no evidence for this transition. In addition, for the $S_2(0)$, expected between 8380 cm^{-1} and 8400 cm^{-1} , no evidence is found (see Fig. 6). Therefore, these kinds of transitions seem to be limited to quadrupole transitions, and we can neglect them for our basic set of selection rules.

3. Second vibrational branch of the H_2 - D_2 mixture

The transitions between the H_2 and D_2 second vibrational branches give a model-free proof for the heteromolecular dimers. The Raman based measurement of the sample isotopologue concentration, before and after the IR measurement, proves that this sample had an HD concentration of less than one percent (see Table 1). Therefore, HD as an origin of the lines in this region can be excluded and leaves heteromolecular dimers as the only cause for this spectral feature. The most obvious lines in the mixture are between 7100 cm^{-1} and 7800 cm^{-1} . These can be assigned to the heteromolecular Q_1Q_1 and S_1Q_1 transitions. The S_1Q_1 transition splits into four different components, depending on the location of the rotational excitation that can occur on a *ortho*- H_2 (at 7700 cm^{-1}),

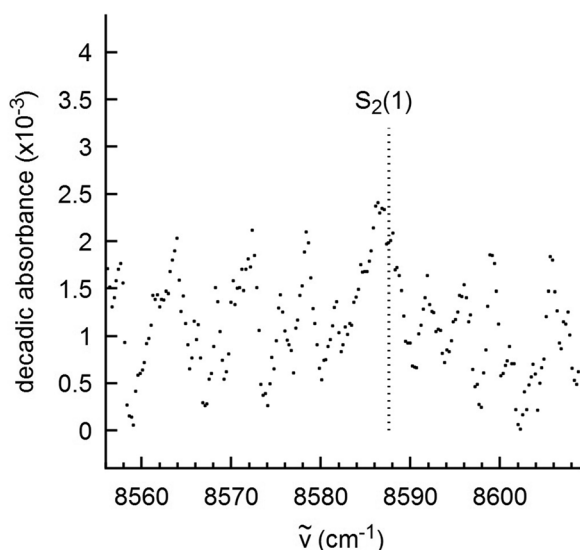


FIG. 5. IR-spectrum of liquid H_2 near the monomer-S-quadrupole transition. The calculated line position is indicated by the annotated dotted line; for further details see text.

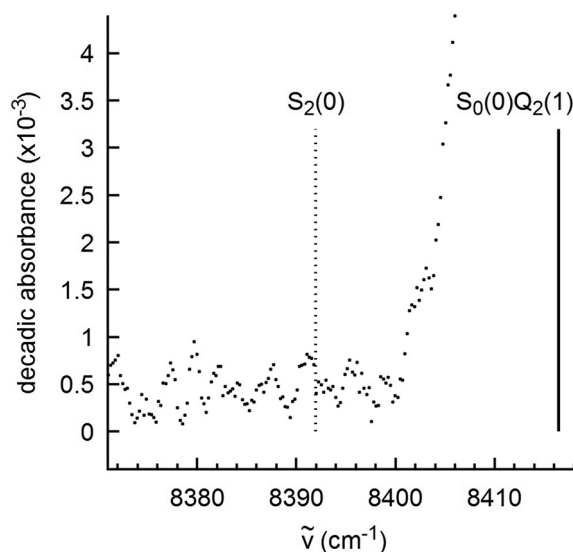


FIG. 6. IR-spectrum of liquid H_2 near the monomer-S-quadrupole transition. Calculated line positions are indicated: dotted line— $S_2(0)$; solid line— $S_0(0)Q_2(1)$.

para- H_2 (at 7500 cm^{-1}), *para*- D_2 (at 7420 cm^{-1}), or *ortho*- D_2 (at 7300 cm^{-1}) molecule.

Within the second vibrational branch of H_2 and D_2 , additional single and double-S transitions with a vibrational excitation of $\Delta v = +2$ are visible.

VI. DISCUSSION

The primary objective of this study is to obtain a minimal but complete set of descriptors for the IR absorption spectra of liquid hydrogen isotopologues. This is mandatory when aiming for an optimized calibration procedure to improve the accuracy from 5% to 1% and to extend our calibration for H_2 , D_2 , and HD mixtures to all six hydrogen isotopologues.

We find that the spectra of homomolecular mixtures are well-described using the following set of descriptors:

- monomer vibrational excitations $\Delta v = +1, +2$ with $Q_{\Delta v}(0, 1)$,
- phonon excitations, 50 cm^{-1} to 100 cm^{-1} higher than the monomer excitations,
- dimer excitations as combinations of $\Delta J_{1,2} = 0, +2$ and $\Delta v_{1,2} = 0, +1, +2$, where each molecule in the dimer must undergo at least one transition.

This set satisfactorily predicts all observed spectral features. However, regarding the integral absorbance, three important effects need to be taken into account.

First, the second vibrational branches are suppressed by one to two orders of magnitude compared to the first vibrational branches. These transitions are only allowed due to the anharmonicity of the vibrational potential and are, therefore, suppressed. For the other transitions, a closer investigation is needed since there is no simple reason that the Q_1Q_1 lines compared to Q_1 are suppressed by the same order of magnitude as Q_2 to Q_1 .

Second, all dimer double-S-transitions are strongly suppressed compared to their corresponding single-S-transitions, but not forbidden. These transitions were identified in the spectra of the first and second vibrational branch and have to be taken into account for a calibration accuracy of about 1% or better. The observed suppression could be explained by the fact that, in a double S-transition, the rotational excitation and the configuration of all three spins (J_A , J_B , and the dimer rotational quantum number l) need to fulfill the photon selection rule of $\Delta J = -1, 0, +1$ in combination. However, precise information about all bound states of the dimers is needed for a full calculation of the phase space of these transitions, which could be gathered by calculations similar to those by Hinde.²²

Third, the missing monomer S-transitions are in agreement with the suppression of quadrupole transitions and, therefore, do not need to be considered for a calibration with an accuracy of 1%. However, from the literature, it is known that these lines can be found in high resolution spectra.^{12,23,37} In order to achieve high precision calibration with an accuracy much better than 1%, these lines need to be investigated in detail as it can be seen for gas phase spectra (see Ref. 38 for HD, Ref. 23 for pure rotational excitation, and Ref. 12 for dimers). It may, therefore, be concluded that the missing dimer transition lines, for which only one molecule exhibits vibration and the dimer itself is rotationally excited ($S_{\Delta\nu}Q_0$), seem to be prohibited or suppressed.

Additionally, various effects complicate the calibration of an IR absorption based measurement system for the isotopologue concentration.

First, the samples are mixtures of all six isotopologues, which complicates the spectra due to additional heteromolecular-dimer lines and overlaps caused by the broad absorption lines in the liquid phase.

Second, the absorbance depends not only on the six isotopologue concentrations, but also on the three ortho/para ratios.³⁹

Third, the underlying physics of this set of selection rules causes mutual influence between the isotopologues and the spin isomer states ortho and para.

This results in a dependence even for the absorbance of the lines of one isotopologue from the concentrations and ortho/para ratios of the other isotopologues. This is due to the fact that the transition matrix elements are induced by molecular interactions with the neighboring molecules;^{18,40–42} therefore, the transitional dipole moment can be described as first order approximation as the product of the polarizability of the absorbing molecule and the field strength of the colliding molecule.^{8,41} The polarizability p_J of the molecules weakly depends (<1%) on the rotational state,⁴³ but the multipole moments F_J of the $J = 0$ and $J = 1$ H₂ molecules differ by two orders of magnitude. Thus, the transition matrix element needs to be a function of both concentrations and surface field strength⁴⁴ following $M_{Q_1(0)}(p_{J_0}, c_{J_0} \cdot F_{J_0}, c_{J_1} \cdot F_{J_1})$. This should be also true for mixtures of H₂ and D₂ and directly leads to the dependence of the integral absorbance of the D₂ Q₁ and Q₂ transition on the H₂ ortho–para ratio and vice versa.

This mechanism can be further investigated by a careful investigation of the dependence of the line absorbance on the ortho–para ratios. The information gathered by highly accurate calibration of the integral absorbance against the isotopologue and ortho–para composition can be combined with the information gathered from line shapes. As shown by Mengel *et al.*,¹³ the differences in line

shapes between the liquid and solid phase allow deep insights into the underlying physics.^{45,46}

The mutual influence between the different isotopologues can also be used to acquire macroscopic information of the sample, such as the homogeneity of the ortho/para and isotopologue distribution in the sample. The ortho/para homogeneity, for example, can be derived from the double S transitions in the first vibrational branch (see Fig. 1, between 3300 cm⁻¹ and 3600 cm⁻¹). For ortho–para lines, the absorbance is at its maximum in a homogeneous sample, while for ortho–ortho and para–para lines, the absorbance is at its minimum. With decreasing homogeneity (corresponding to a physical separation of the ortho and para molecules in the sample), the possibility to find ortho–para dimers will decrease and the absorbance of the ortho–ortho and para–para lines will increase. As a consequence, one may be able to determine the homogeneity from the relative absorbance of these lines. The same method can be used to determine the homogeneity of the isotopologue composition, where pure H₂ or pure D₂ transitions can be compared to the transitions of H₂–D₂ dimers. However, only a careful investigation and calibration at the 1% level can give more detailed information about the liquid state and the underlying physics. An application of this can be of interest when studying phase transitions from liquid to solid where the solubility of one of the molecules can be different in the one or the other phase.

VII. CONCLUSION

The prediction of detailed line absorbance needs the calculation of transitional matrix elements, which are not available at the present time. However, there are some calculations for solid para-hydrogen absorption coefficients⁴⁷ and a six-dimensional potential surface for ground state H₂ and D₂ dimers. A full set of absorption coefficients for the liquid phase would be appreciated and combined with the data here, enabling detailed studies of the interaction processes in the liquid phase of hydrogen isotopologues.

However, with the basic set of selection rules of $\Delta\nu \geq 0$ and $\Delta J = 0, \pm 2$, we are able to sufficiently describe the first and second vibrational branches of liquid hydrogen IR absorption spectra of pure H₂, pure D₂, and H₂–D₂ mixtures.

We are confident that this set also describes mixtures with the other four isotopologues, including the tritiated species.^{48–50} This will be verified with the new tritium compatible setup TApIR 2 currently under construction.⁴ The selection rules will also allow us to develop an optimized strategy for a calibration with an improved accuracy of 1% or better.

The main systematic effect in this procedure is expected to be the ortho/para ratios of the three homonuclear isotopologues. Therefore, one should think of the ortho and para molecules as fully distinguishable species in the liquid phase. In conclusion, the parameter space for a full calibration will contain nine parameters, one for each of the heteronuclear molecules and two for each of the homonuclear molecules.

Further studies of the liquid should address in more detail the dependence of the absorbance on the ortho–para and isotopologue composition, instead of the line positions, which are not an ideal parameter in the liquid phase. Future work should also try to deconvolute the lines according to the identified underlying transitions that contribute to the observed line features. Specifically, the change

during the ortho–para conversion promises a clear and testable deconvolution of several lines, such as the double-S-transitions in the first vibrational branch, the collision induced Q₂ monomer lines, and the pure vibrational and single S dimer lines in the second vibrational branch. Combined with an accurate calibration, this will enable investigations of the liquid phase itself to gain a deeper understanding of liquid hydrogen.

DATA AVAILABILITY

Data files of the spectra shown in this publication are available from the corresponding author upon reasonable request.

SUPPLEMENTARY MATERIAL

See the [supplementary material](#) for the complete list of calculated transitions in the investigated region.

REFERENCES

- ¹A. Watanabe and H. L. Welsh, “Direct spectroscopic evidence of bound states of (H₂)₂ complexes at low temperatures,” *Phys. Rev. Lett.* **13**, 810–812 (1964).
- ²R. Größle, A. Beck, B. Bornschein, S. Fischer, A. Kraus, S. Mirz, and S. Rupp, “First calibration measurements of an FTIR absorption spectroscopy system for liquid hydrogen isotopologues for the isotope separation system of fusion power plants,” *Fusion Sci. Technol.* **67**, 357–360 (2015).
- ³R. Größle, A. Kraus, S. Mirz, and S. Wozniowski, “First calibration of an IR absorption spectroscopy system for the measurement of H₂, D₂, and HD concentration in the liquid phase,” *Fusion Sci. Technol.* **71**, 369–374 (2017).
- ⁴S. Mirz, U. Besserer, B. Bornschein, R. Größle, B. Krasch, and S. Welte, “Design of a spectroscopy experiment for all hydrogen isotopologues in the gaseous, liquid, and solid phase,” *Fusion Sci. Technol.* **71**, 375–380 (2017).
- ⁵A. R. W. McKellar and M. J. Clouter, “Infrared spectra of liquid hydrogen and deuterium,” *Can. J. Phys.* **72**, 51–56 (1994).
- ⁶G. Varghese, R. D. G. Prasad, and S. P. Reddy, “Absorption spectra of solid para- and normal hydrogen in the first overtone region,” *Phys. Rev. A* **35**, 701–707 (1987).
- ⁷Y. Yonezawa and T. Fueno, “Semi-classical calculation of the vibrational transition probabilities of diatomic molecules in collision. The effect of vibrational anharmonicity,” *Bull. Chem. Soc. Jpn.* **44**, 2976–2980 (1971).
- ⁸J. van Kranendonk, “Theory of induced infra-red absorption,” *Physica* **23**, 825–837 (1957).
- ⁹G. Herzberg, *Molecular Spectra and Molecular Structure, Infrared and Raman Spectra of Polyatomic Molecules Vol. 2* (Krieger Publishing, Malabar, 1991).
- ¹⁰I. V. Hertel, C.-P. Schulz, I. V. Hertel, and C.-P. Schulz, *Atome, Moleküle und Optische Physik 1: Atomphysik und Grundlagen der Spektroskopie*, edited by I. V. Hertel and C.-P. Schulz, Springer-Lehrbuch Springer Link: Bücher (Springer Berlin Heidelberg, Berlin, Heidelberg, 2008).
- ¹¹H. P. Gush, E. J. Allin, H. L. Welsh, and W. F. J. Hare, “The infrared fundamental band of liquid and solid hydrogen,” *Can. J. Phys.* **38**, 176–193 (1960).
- ¹²A. R. W. McKellar, “Infrared spectra of hydrogen dimers,” *J. Chem. Phys.* **92**, 3261–3277 (1990).
- ¹³M. Mengel, B. P. Winnewisser, and M. Winnewisser, “Overtone spectra of parahydrogen and orthodeuterium in the liquid phase,” *Can. J. Phys.* **78**, 317–325 (2000).
- ¹⁴G. Bachet, E. R. Cohen, P. Dore, and G. Birnbaum, “The translational–rotational absorption spectrum of hydrogen,” *Can. J. Phys.* **61**, 591–603 (1983).
- ¹⁵T. K. Balasubramanian, C.-H. Chen-Hsin Lien, J. R. Gaines, K. Narahari Rao, E. K. Damon, and R. J. Nordstrom, “Infrared spectrum of hydrogen in the condensed phase with high-sensitivity spectrometers: Experiments with a 0.04 cm⁻¹ Fourier transform spectrometer in the range 1.5–12 μm,” *J. Mol. Spectrosc.* **92**, 77–84 (1982).
- ¹⁶J. P. Bouanich, C. Brodbeck, P. Drossart, and E. Lellouch, “Collision-induced absorption for H₂–H₂ and H₂–He interactions at 5 μm,” *J. Quant. Spectrosc. Radiat. Transfer* **42**, 141–147 (1989).
- ¹⁷A. Campargue, S. Kassi, K. Pachucki, and J. Komasa, “The absorption spectrum of H₂: CRDS measurements of the (2–0) band, review of the literature data and accurate *ab initio* line list up to 35 000 cm⁻¹,” *Phys. Chem. Chem. Phys.* **14**, 802–815 (2012).
- ¹⁸G. E. Ewing and S. Trajmar, “Induced infrared absorption of solutions of H₂ and D₂ in liquid neon,” *J. Chem. Phys.* **42**, 4038–4046 (1965).
- ¹⁹J. van Kranendonk, “Rotational and vibrational energy bands in solid hydrogen,” *Physica* **25**, 1080–1094 (1959).
- ²⁰J. Van Kranendonk and G. Karl, “Theory of the rotational and vibrational excitations in solid parahydrogen, and frequency analysis of the infrared and Raman spectra,” *Rev. Mod. Phys.* **40**, 531–555 (1968).
- ²¹K. Hyeon-Deuk and K. Ando, “Intermolecular diatomic energies of a hydrogen dimer with non-Born-Oppenheimer nuclear and electron wave packets,” *Chem. Phys. Lett.* **532**, 124–130 (2012).
- ²²R. J. Hinde, “A six-dimensional H₂–H₂ potential energy surface for bound state spectroscopy,” *J. Chem. Phys.* **128**, 154308 (2008).
- ²³A. R. W. McKellar and J. Schaefer, “Far-infrared spectra of hydrogen dimers: Comparisons of experiment and theory for (H₂)₂ and (D₂)₂ at 20 K,” *J. Chem. Phys.* **95**, 3081–3091 (1991).
- ²⁴C. Kim, S. J. Kim, Y. Lee, and Y. Kim, “Quantum mechanical study of van der Waals complex. I. The H₂ dimer using the DFT and the multi coefficient G2/G3 methods,” *Bull. Korean Chem. Soc.* **21**, 510–514 (2000), available at <http://www.koreascience.or.kr/article/JAKO200013464476674.org>.
- ²⁵P. Souers, *Hydrogen Properties for Fusion Energy* (University of California Press, 1986).
- ²⁶A. H. Larsen, F. E. Simon, and C. A. Swenson, “The rate of evaporation of liquid hydrogen due to the ortho–para hydrogen conversion,” *Rev. Sci. Instrum.* **19**, 266–269 (1948).
- ²⁷Y. Y. Milenko and R. M. Sibileva, “Natural ortho–para conversion rate in liquid and gaseous hydrogen,” *J. Low Temp. Phys.* **107**, 77–92 (1997).
- ²⁸M. Schlösser, B. Bornschein, S. Fischer, T. M. James, F. Kassel, S. Rupp, M. Sturm, and H. H. Telle, “Raman spectroscopy at the Tritium Laboratory Karlsruhe,” *Fusion Sci. Technol.* **67**, 555–558 (2015).
- ²⁹M. Sturm, M. Schlösser, R. J. Lewis, B. Bornschein, G. Drexlin, and H. H. Telle, “Monitoring of all hydrogen isotopologues at Tritium Laboratory Karlsruhe using Raman spectroscopy,” *Laser Phys.* **20**, 493–507 (2010).
- ³⁰I. K. Mikhailyuk and A. P. Razzhivin, “Background subtraction in experimental data arrays illustrated by the example of Raman spectra and fluorescent gel electrophoresis patterns,” *Instrum. Exp. Tech.* **46**, 765–769 (2003).
- ³¹K. P. Huber and G. Herzberg, *Molecular Spectra and Molecular Structure: IV. Constants of Diatomic Molecules* (Van Nostrand Reinhold Company, 1979).
- ³²E. J. Allin, W. F. J. Hare, and R. E. MacDonald, “Infrared absorption of liquid and solid hydrogen,” *Phys. Rev.* **98**, 554–555 (1955).
- ³³D. H. Weitzel, W. V. Loebenstein, J. W. Draper, and O. E. Park, “Ortho–para catalysis in liquid-hydrogen production,” *J. Res. Natl. Bur. Stand.* **60**, 221–227 (1958).
- ³⁴Reminder: The J = 0 state corresponds to para H₂ or ortho D₂.
- ³⁵S. Kassi and A. Campargue, “Electric quadrupole transitions and collision-induced absorption in the region of the first overtone band of H₂ near 1.25 μm,” *J. Mol. Spectrosc.* **300**, 55–59 (2014).
- ³⁶S. Kassi, A. Campargue, K. Pachucki, and J. Komasa, “The absorption spectrum of D₂: Ultrasensitive cavity ring down spectroscopy of the (2–0) band near 1.7 μm and accurate *ab initio* line list up to 24 000 cm⁻¹,” *J. Chem. Phys.* **136**, 184309 (2012).
- ³⁷G. Danby, “Theoretical studies of van der Waals molecules: The D₂–D₂ dimer,” *J. Phys. B: At., Mol. Opt. Phys.* **22**, 1785 (1989).
- ³⁸S. Kassi and A. Campargue, “Electric quadrupole and dipole transitions of the first overtone band of HD by CRDS between 1.45 and 1.33 μm,” *J. Mol. Spectrosc.* **267**, 36–42 (2011).
- ³⁹W. F. J. Hare, E. J. Allin, and H. L. Welsh, “Infrared absorption of liquid and solid hydrogen with various ortho–para ratios,” *Phys. Rev.* **99**, 1887–1888 (1955).

- ⁴⁰G. E. Ewing and S. Trajmar, "Infrared induced absorption of dilute solutions of H₂ and D₂ in liquid argon," *J. Chem. Phys.* **41**, 814–819 (1964).
- ⁴¹J. B. Nelson and G. C. Tabisz, "Intracollisional interference in the pure rotational spectrum of HD: Determination of the permanent electric dipole moment," *Phys. Rev. A* **28**, 2157–2161 (1983).
- ⁴²J. Schaefer, "Dimer features of H₂–H₂ and isotopomers at low temperatures," in *Collision- and Interaction-Induced Spectroscopy*, NATO ASI Series Vol. 452, edited by G. Tabisz and M. Neuman (Springer Netherlands, 1995), pp. 485–494.
- ⁴³C. Schwartz and R. J. Le Roy, "Nonadiabatic eigenvalues and adiabatic matrix elements for all isotopes of diatomic hydrogen," *J. Mol. Spectrosc.* **121**, 420–439 (1987).
- ⁴⁴M. Zoppi, L. Ulivi, M. Santoro, M. Moraldi, and F. Barocchi, "Density behavior of the double rotational transition in liquid parahydrogen," *Phys. Rev. A* **53**, R1935–R1938 (1996).
- ⁴⁵K. Yoshioka, P. L. Raston, and D. T. Anderson, "Infrared spectroscopy of chemically doped solid parahydrogen," *Int. Rev. Phys. Chem.* **25**, 469–496 (2006).
- ⁴⁶A. Crane and H. P. Gush, "The induced infrared absorption spectrum of solid deuterium and solid hydrogen deuteride," *Can. J. Phys.* **44**, 373–398 (1966).
- ⁴⁷R. J. Hinde, "Absorption intensity of the Q₁(0) + Q₁(0) and Q₁(0) + Q₂(0) double vibrational transitions in solid parahydrogen," *Phys. Rev. B* **61**, 11451–11453 (2000).
- ⁴⁸P. C. Souers, D. Fearon, R. Garza, E. M. Kelly, P. E. Roberts, R. H. Sanborn, R. T. Tsugawa, J. L. Hunt, and J. D. Poll, "Infrared spectra of liquid and solid DT and T₂," *J. Chem. Phys.* **70**, 1581–1584 (1979).
- ⁴⁹P. C. Souers, J. Fuentes, E. M. Fearon, P. E. Roberts, R. T. Tsugawa, J. L. Hunt, and J. D. Poll, "Infrared spectra of liquid and solid HT and HD in mixtures with T₂," *J. Chem. Phys.* **72**, 1679–1684 (1980).
- ⁵⁰P. C. Souers, E. M. Fearon, P. E. Roberts, R. T. Tsugawa, J. D. Poll, and J. L. Hunt, "Collision induced infrared lines in solid hydrogens caused by tritium radioactivity," *Phys. Lett. A* **77**, 277–280 (1980).